Copper(II) and Nickel(II) Complexes of Binucleating Macrocyclic Bis(disulfide)tetramine Ligands

Stephen Fox,† Robert T. Stibrany, Joseph A. Potenza,* Spencer Knapp,* and Harvey J. Schugar*

Department of Chemistry, Rutgers, The State University of New Jersey, 610 Taylor Road, Piscataway, New Jersey 08854-8087

Received April 10, 2000

Novel macrocyclic bis(disulfide)tetramine ligands and several Cu(II) and Ni(II) complexes of them with additional ligands have been synthesized by the oxidative coupling of linear tetradentate N_2S_2 tetramines with iodine. Facile demetalation of the Ni(II) oxidation products affords the free 20-membered macrocycles *meso*-**9** and *rac*-**9** and the 22-membered macrocycle **16**, all of which are potentially octadentate N_4S_4 ligands. X-ray structure analyses reveal distinctly different conformations for the two isomers of **9**; *meso*-**9** shows a stepped conformation in profile with the disulfide groups corresponding to the rise of the step, whereas *rac*-**9** exhibits a V conformation with the disulfide groups near the vertex of the V. No metal complexes of *rac*-**9** have been isolated. Crystallographic studies of three Cu(II) complexes reveal that depending upon the size of the macrocyclic ligand and the nature of the additional ligands (I^-, *N*CO^-, and CH_3CN), the Cu(II) coordination geometry shows considerable variation (plasticity), with substantial changes in the Cu(II)−disulfide bonding. Thus, a diiodide salt contains six-coordinate Cu(II) to which all four bridging disulfide sulfur atoms form strong equatorial bonds. In contrast, isocyanato complexes of the 20- and 22-membered macrocycles exhibit trigonal-bipyramidal Cu(II) and distorted cis-octahedral Cu(II) geometries, respectively, having only one and no short equatorially bound sulfur atoms. The coordination geometry of the latter complex can also be described as four-coordinate seesaw with two semicoordinated S(disulfide) ligands. Disulfide → Cu(II) ligand-to-metal charge transfer absorptions of both isocyanato-containing Cu(II) species appear too weak to observe, probably because of poor overlap of the sulfur orbitals with the Cu(II) d-vacancy. The dual disulfide-bridged Ni(II) units of the crystallographically characterized octahedral Ni(II) complex of *meso*-**9** with axial iodide and acetonitrile ligands promote substantial antiferromagnetic coupling ($J = -13.0(2)$ cm^{-1}).

Introduction

The extensive literature of mixed-donor macrocyclic ligands[1] includes, to our knowledge, only one example in which a metal ion is bound to the disulfide incorporated in the macrocycle. Although cystine cross-linked peptides constitute an enormous class of macrocycles containing one or more disulfide groups, the ligating roles of such disulfide units have apparently been neither demonstrated nor widely investigated.[2] For example, the possibility of copper−disulfide bonding for stellacyanin has been removed by spectroscopic[3] and crystallographic[4] studies. Cu(II)−disulfide interactions have been reported for a polymeric complex[5] and for four binuclear complexes having Cu(II) ions bridged by penicillamine disulfide,[6] oxidized glutathione,[7] cystine,[8] and μ-η^2:η^2 S_2.[9] Strong metal−macrocyclic disulfide bonding has been characterized for the Os(II) complex of a 14-membered macrocycle having diphosphinobis(disulfide) donors along with pendant thiolate groups.[10] Disulfide-bridged Ir_2^{6+},[11a] Rh_2^{6+},[11b] and Ni_2^{4+} [12] species and mononuclear Ni(II) disulfide bonding[13] have been reported for linear disulfide-containing ligands. Metal-free cyclic disulfides[14] and bis- and tris(disulfides)[15] have been characterized, and potentially ligating cyclic disulfides elaborated with N-donors are known.[16] In this paper, we report metal ion template syntheses of new binucleating

† Current address: Department of Chemistry, University of Louisiana at Monroe, Monroe, LA 71209.

(1) Bowman-James, K. In *Encyclopedia of Inorganic Chemistry*; King, R. B., Ed.; Wiley: New York, 1994; Vol. 4, pp 1999−2016 and references therein.
(2) Danyi, P.; Várnagy, K.; Sóvágó, I.; Schön, I.; Sanna, D.; Micera, G. *J. Inorg. Biochem.* **1995**, *60*, 69−78.
(3) Thomann, H.; Bernardo, M.; Baldwin, M. J.; Lowery, M. D.; Solomon, E. I. *J. Am. Chem. Soc.* **1991**, *113*, 5911−3.
(4) Hart, P. J.; Nerissian, A. M.; Herrmann, R. G.; Nalbandyan, R. M.; Valentine, J. S.; Eisenberg, D. *Protein Sci.* **1996**, *5*, 2175−83.
(5) Brader, M. L.; Ainscough, E. W.; Baker, E. N.; Brodie, A. M.; Lewandoski, D. A. *J. Chem. Soc., Dalton Trans.* **1990**, 2089−94.
(6) Thich, J. A.; Mastropaolo, D.; Potenza, J.; Schugar, H. J. *J. Am. Chem. Soc.* **1974**, *96*, 726−31.
(7) Miyoshi, K.; Sugiura, Y.; Ishizu, K.; Iitaka, Y.; Nakamura, H. *J. Am. Chem. Soc.* **1980**, *102*, 6130−6.
(8) Gutiérrez, J. N.; Garcia, E. A.; Viossat, B.; Dung, N. H.; Busnot, A.; Hemidy, J. F. *Acta Crystallogr.* **1993**, *C49*, 19−22 and references therein.
(9) Fujisawa, K.; Moro-oka, Y.; Kitajima, N. *J. Chem. Soc., Chem. Commun.* **1994**, 623−4.
(10) Dilworth, J. R.; Zheng, Y.; Miller, J. R. *J. Chem. Soc., Dalton Trans.* **1992**, 1757−8.
(11) (a) Konno, T.; Miyashita, Y.; Okamoto, K.-i. *Chem. Lett.* **1997**, 85−6. (b) Miyashita, Y.; Sakagami, N.; Yamada, Y.; Konno, T.; Okamoto, K. *Bull. Chem. Soc. Jpn.* **1998**, *71*, 2153−60.
(12) Handa, M.; Mikuriya, M.; Ōkawa, H. *Chem. Lett.* **1989**, 1663−6.
(13) Riley, P. E.; Seff, K. *Inorg. Chem.* **1972**, *11*, 2993−9.
(14) (a) Bhattacharya, S.; Ghosh, S.; Easwaran, K. R. K. *J. Org. Chem.* **1998**, *63*, 9232−42. (b) Ranganathan, D.; Lakshmi, C.; Karle, I. L. *J. Am. Chem. Soc.* **1999**, *121*, 6103−7.
(15) (a) Houk, J.; Whitesides, G. M. *Tetrahedron* **1989**, *45*, 91−102 and references therein. (b) Tam-Chang, S.-W.; Stehouwer, J. S.; Hao, J. *J. Org. Chem.* **1999**, *64*, 334−5.

10.1021/ic000380p CCC: $19.00
Published on Web 09/28/2000

Scheme 1. Synthesis of Diaminocyclohexane Based Ligands and Complexes

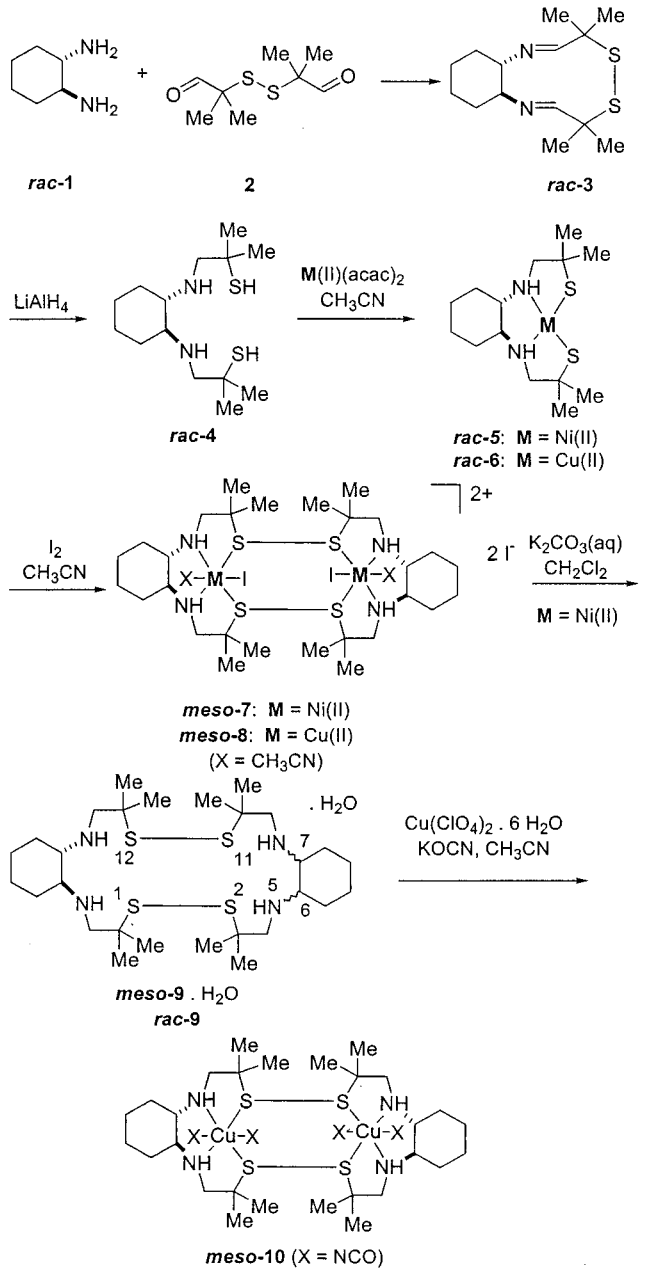

Scheme 2. Synthesis of 2,2-Dimethyl-1,3-propylidene Based Ligands and Complexes

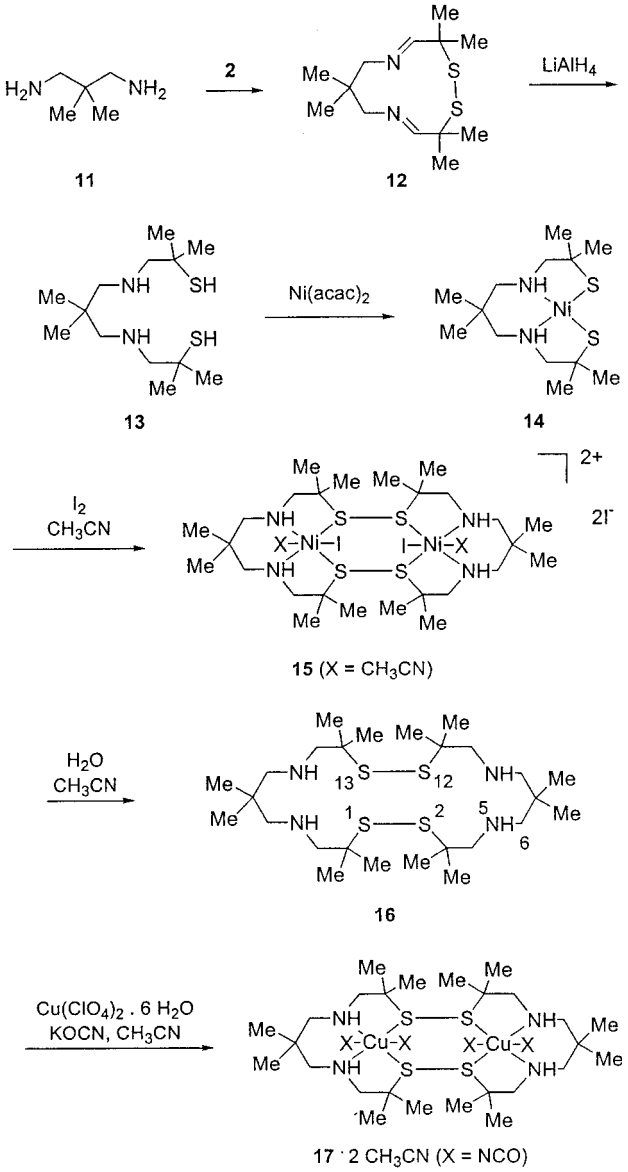

macrocyclic bis(disulfide)tetramine ligands along with structural, spectroscopic, and magnetochemical studies of their Cu(II) and Ni(II) complexes.[17] Complexes of these potentially octadentate macrocyclic ligands feature prominent M(II)−disulfide interactions and disulfide superexchange pathways.

Experimental Section

General Procedures and Methods. Unless otherwise noted, reagents were obtained from commercial suppliers and were used as received. Reactions were carried out in vessels open to the atmosphere unless otherwise noted. Conventional electronic spectral measurements were made using a Cary spectrophotometer that was upgraded and computer-interfaced by Aviv Associates. The magnetic susceptibilities of **7** and **10** were measured over the 10−300 K range using a Quantum Design SQUID magnetometer operated at an applied field of 1000 G. Diamagnetic corrections were calculated from Pascal's constants and applied to the susceptibilities. ^{1}H and ^{13}C NMR spectra were obtained by using chloroform solutions unless otherwise noted. Chemical shifts are reported in ppm downfield from the internal tetramethylsilane signal, and coupling constants *J* are in hertz. Organic solutions were dried over anhydrous sodium sulfate.

Preparation of the Complexes. The synthetic routes used to prepare the bis(disulfide) macrocycles **9** and **16** and several of their Ni(II) and Cu(II) complexes are outlined in Scheme 1 (**9a** and its complexes **7**, **8**, and **10**) and Scheme 2 (**16** and its complexes **15** and **17**).

Bis(2-methyl-1-oxo-2-propyl)disulfide (2). Compound **2** was prepared by modification of a literature procedure.[18] A solution of 230 mL (2.53 mol) of distilled isobutyraldehyde in 260 mL of carbon tetrachloride was stirred under a nitrogen atmosphere at 40 °C. Sulfur monochloride, S_2Cl_2 (135 g, 1 mol), was added dropwise, while maintaining the temperature between 40 and 50 °C. After 2 h, the

(16) (a) Sondhi, S. M.; Kolodziejczyk, P.; Ball, R. G.; Lown, J. W. *J. Org. Chem.* **1988**, *53*, 4310−4. (b) Maharajh, R. B.; Snyder, J. P.; Britten, J. F.; Bell, R. A. *Can. J. Chem.* **1997**, *75*, 140−61. (c) Lai, C.-H.; Reibenspies, J. H.; Darensbourg, M. Y. *J. Chem. Soc., Chem. Commun.* **1999**, 2473−4.

(17) A preliminary report of some of this work has appeared. See: Fox, S.; Potenza, J. A.; Knapp, S.; Schugar, H. J. In *Bioinorganic Chemistry of Copper*; Karlin, K. D., Tykelár, Z., Eds.; Chapman & Hall: New York, 1993; pp 34−47.

(18) D'Amico, J. J.; Dahl, W. E. *J. Org. Chem.* **1975**, *40*, 1224−7.

reaction was cooled and concentrated to afford a yellow oil, which was dissolved in ether. The organic solution was washed with water, dried, concentrated, and then distilled at 1 mmHg and 120 °C to afford 156.7 g (76%) of **2** as a straw-colored oil.

3*S,4*S**-2,5-Diaza-9,10-dithia-7,7,10,10-tetramethyl-perhydrobenzo-[*c*]cyclodec-1*E*,5*E*-diene (*rac*-3).** A solution of 9.14 g (80 mmol) of *rac*-*trans*-1,2-diaminocyclohexane (Aldrich) and 16.8 g (80 mmol) of α,α′-dithiodiisobutyraldehyde (**2**) in 150 mL of hexane was heated at reflux for 2 h in a flask fitted with a Dean−Stark water trap. The solution was filtered hot and then allowed to cool to room temperature. The resulting colorless rectangular plates were collected by filtration, washed with cold hexane and then acetone, and then dried in air to afford 13.4 g (59%) of *rac*-**3**, mp 144−145 °C: IR (KBr) 1664 cm^{-1}; ^{13}C NMR (20 MHz) 165.17 (*C*═N), 52.76, 31.33, 24.49, 24.37, 21.25; ^1H NMR (400 MHz) 6.97 (s, 2 H), 2.75−2.89 (m, 2 H), 1.96 (app d, J = 12, 2 H), 1.68−1.86 (m, 4 H), 1.22−1.48 (m, 2 H), 1.44 (s, 6 H), 1.33 (s, 6 H). The macrocyclic Schiff base *rac*-**3** was further characterized by X-ray crystallography.[19]

***trans*-*rac*-*N*,*N*′-Bis(2-mercapto-2-methylprop-1-yl)-1,2-cyclohexanediamine (*rac*-4).** A solution of 5 g (17 mmol) of *rac*-**3** in 100 mL of dry tetrahydrofuran was added dropwise to a stirred suspension of 1.31 g (34 mmol) of lithium aluminum hydride in 20 mL of tetrahydrofuran at −78 °C. The mixture was warmed to room temperature, heated at reflux for 12 h, cooled, quenched by dropwise addition of 10 mL of saturated aqueous sodium sulfate, combined with 100 mL of diethyl ether, and then filtered. The filtrate was dried and then concentrated to give 3.6 g (72%) of crude *rac*-**4** as a colorless oil, which was stored at −10 °C under nitrogen. This compound decomposes over time and is best used promptly: ^{13}C NMR (100 MHz) 61.76 (N−*C*H_2−), 60.21 (N−*C*H−), 44.89 (4° *C*−SH), 31.21 (two ring *C*H_2 groups), 30.04 and 29.89 (two diastereotopic Me pairs), 24.34 (two ring *C*H_2 groups); ^1H NMR (400 MHz) 2.82 and 2.45 (AB quartet, J = 12, 4 H, N−CH_2), 2.14−2.30 (m, 2 H), 1.88−2.14 (m, 6 H), 1.65−1.79 (m, 2 H), 1.39 (s, 6 H), 1.37 (s, 6 H), 1.18−1.27 (m, 2 H), 0.90−1.13 (m, 2 H).

***trans*-*rac*- *N*,*N*′-Bis(2-mercapto-2-methylprop-1-yl)-1,2-cyclohexanediaminenickel(II) (*rac*-5).** A solution of 6.47 g (22.3 mmol) of *rac*-**4** in 20 mL of acetonitrile was added to a suspension of 5.00 g (19.45 mmol) of nickel(II) acetylacetonate, Ni(acac)$_2$, in 50 mL of acetonitrile, and the resulting brown solution was stirred overnight. A brown pasty solid was collected by filtration, washed with acetonitrile (3 × 10 mL), and then dried in vacuo to give 5.67 g of crude nickel complex *rac*-**5** (84%), mp (dec) >310 °C: ^{13}C NMR (400 MHz, CD_3CN) 65.13, 63.32, 45.64, 32.18, 30.32, 29.49, 23.18; ^1H NMR (400 MHz, CD_3CN) 3.03 (br m, 2 H), 2.70 (d, J = 8.0, 2 H), 2.49 (br m, 2 H), 2.41 (t, J = 11.4, 2 H), 2.05 (br d, J = 6.2, 2 H), 1.67 (br m, 2 H), 1.27 (br s, 6 H), 1.24 (br s, 6 H), 1.10 (br s, 2 H), 1.09 (br s, 2 H).

***trans*- *N*,*N*′-Bis(2-mercapto-2-methylprop-1-yl)-1,2-cyclohexanediaminecopper(II) (*rac*-6).** A solution of 1.4 g (4.8 mmol) of *rac*-**4** in 10 mL of acetonitrile was added to a flask containing 0.75 g (2.9 mmol) of copper(II) acetylacetonate, Cu(acac)$_2$. The resulting mixture of deep red solution and dark precipitate was stirred and heated at 70 °C for 10 min and then cooled at −20 °C for 1 h. The black crystalline product was collected by filtration, washed with ether, and then dried in air to afford 0.85 g of crude *rac*-**6** (83% based on copper), mp 198−199 °C. Anal. Calcd (Found) for $CuS_2N_2C_{14}H_{28}$: Cu, 18.04 (15.7); S, 18.21 (18.35); N, 7.96 (8.07); C, 47.76 (47.85); H, 8.02 (7.85). Complex *rac*-**6** was fully characterized structurally and spectroscopically; details will be reported elsewhere.[20a]

$[Ni_2(9a)(2I)(CH_3CN)_2]^{2+}2I^-$ (*meso*-7). A stirred suspension of 2.00 g (5.76 mmol) of *rac*-**5** in 50 mL of acetonitrile was treated with a solution of 1.46 g (5.76 mmol) of iodine in 60 mL of acetonitrile, and the resulting red mixture was filtered and then allowed to stand overnight. Large well-formed green crystals were collected, washed with 20 mL of acetonitrile, and air-dried, affording 3.14 g (85%) of green bipyramidal crystals of *meso*-**7**. Anal. Calcd (Found) for $C_{32}H_{62}N_6S_4I_4Ni_2$: C, 29.93 (30.12); H, 4.87 (4.84); N, 6.54 (6.54); S, 9.99 (9.98); I, 39.53 (39.52); Ni, 9.14 (9.14).

$[Cu_2(9a)I_2(CH_3CN)_2]^{2+}2I^-$ (*meso*-8). A solution of 0.254 g (1 mmol) of iodine in 25 mL of acetonitrile was added to a solution of 0.352 g (1 mmol) of *rac*-**6** in 25 mL of acetonitrile. The resulting red-green solution was filtered and allowed to stand. After 2 days, a black crystalline solid was collected by decantation, washed with acetonitrile, and then dried in air to afford 0.356 g (52%) of the complex *meso*-**8**. Diffraction-quality crystals were obtained by recrystallization from acetone/toluene.

6*S,7*S**,16*R**,17*R**-3,3,10,10,13,13,20,20-Octamethyl-diperhydrobenzo-[*f*,*p*]-1,2,10,12-tetrathia-5,8,15,18-tetraaza-cycloeicosane Monohydrate (*meso*-9·H_2O) and 6*S**,7*S**,16*S**,17*S**-3,3,10,10,13,13,20,20-Octamethyl-diperhydrobenzo [*f*,*p*]-1,2,10,12-tetrathia-5,8,15,18-tetraaza-cycloeicosane (*rac*-9).** Complex *meso*-**7** (809 mg) was demetalated by stirring for 2 h with a mixture of 35 mL of dichloromethane and 35 mL of 5% aqueous potassium carbonate. The mixture at this point consisted of a cloudy pale green aqueous layer and a pale yellow dichloromethane layer. The aqueous layer was extracted twice with 10 mL of dichloromethane, and the combined extract was concentrated to 5 mL. Seven milliliters of acetonitrile was added, and the solution was allowed to evaporate slowly at room temperature. Clumped clear prisms of *rac*-**9** and large flat square plates of *meso*-**9**·H_2O, each suitable for crystallographic characterization, were physically separated to give 130 mg of *meso*-**9**·H_2O (34.7%) and 201.5 mg of *rac*-**9** (55.4%).

***meso*-9·H_2O:** mp 98−99 °C; ^{13}C NMR (400 MHz, CD_2Cl_2) 61.72, 56.23, 49.66, 31.23, 26.38, 25.77, 24.38; ^1H NMR (400 MHz, CD_2Cl_2) 2.63 (d, J = 12.1, 4 H), 2.34 (d, J = 12.1, 4 H), 2.05 (m, 4 H), 1.93 (d, J = 13.4, 4 H), 1.82 (br s, N−H, 4 H), 1.60 (m, 4 H), 1.23 (s, 12 H), 1.19 (s, 12 H), 1.13 (m, 4 H), 0.88 (br m, 4 H); IR (KBr) 2927, 2919 (s), 2850, 1464, 1457, 1116, 1108 cm^{-1}.

***rac*-9**: mp 114−117 °C; ^{13}C NMR (400 MHz) 62.52, 57.18, 50.56, 31.88, 27.09, 26.50, 25.07; ^1H NMR (400 MHz) 2.72 (d, J = 12.1, 4 H), 2.41 (d, J = 12.1, 4 H), 2.13 (d, J = 9.1, 4 H), 2.03 (d, J = 13.1, 4 H), 1.78 (br s, 4 N−H), 1.68 (d, J = 8.1, 4 H), 1.33 (s, 12 H), 1.29 (s, 12 H), 1.20 (br t, J = 10.0, 4 H), 0.97 (br m, 4 H).

Cu_2(*meso*-9)$(NCO)_4$ (*meso*-10). A paste was prepared by mixing 0.048 g (0.6 mmol) of potassium cyanate, 0.5 mL of water, and 0.111 g (0.3 mmol) of $Cu(ClO_4)_2·6H_2O$. The paste was treated with 10 mL of acetonitrile, and this solution was immediately filtered into a filtered solution containing 0.100 g (0.15 mmol) of *meso*-**9**·H_2O in 15 mL of warm acetonitrile. The resulting green solution rapidly deposited a green solid. The mixture was stirred for 15 min, and the solid was collected by filtration, washed with 5 mL of acetonitrile, and dried in vacuo to afford 0.071 g (55%) of *meso*-**10**. Diffraction-quality green crystals were grown by slow diffusion in a test tube in which the lower layer consisted of a solution of $Cu(ClO_4)_2·6H_2O$ and KOCN in acetonitrile and the upper layer was an acetonitrile solution of macrocycle *meso*-**9**. *Caution*: perchlorate-containing compounds may explode if heated or dried.

1,8-Diaza-4,5-dithia-3,3,6,6,10,10-hexamethyl-cycloundeca-1*E*,7*E*-diene (12). A solution of 5.11 g (51 mmol) of 2,2′-dimethyl-1,3-diaminopropane (**11**) and 10.6 g (51 mmol) of freshly distilled dialdehyde **2** in 100 mL of heptane was heated at reflux under a nitrogen atmosphere for 6 h. The reaction mixture was cooled and concentrated to afford 13.8 g (nearly quantitative crude yield) of an orange oil (**12**) that was used immediately in the preparation of **13**: ^{13}C NMR (100 MHz) 169.62 (*C*═N), 71.83 (*C*H_2N), 50.30 (4° *C*−S), 32.35 (4° *C*−CH_3), 26.74 (4° C−*C*H_3), 24.70 and 24.22 (*C*H_3−C−S); ^1H NMR (400 MHz) 7.59 (s, 2 H), 3.28 (s, 4 H), 1.50 (s, 6 H), 1.32 (s, 6 H), 1.17 (s, 6 H).

***N*,*N*′-Bis-(2-methyl-2-mercaptoprop-1-yl)-1,3-diamino-2,2-dimethylpropane (13).** A solution of 13.8 g (50 mmol) of disulfide **12** in 100 mL of tetrahydrofuran was added carefully to a suspension of 2.26 g (69 mmol) of lithium aluminum hydride in 100 mL of dry tetrahydrofuran. The mixture was heated at reflux for 12 h, cooled to −78 °C by use of a dry ice/acetone bath, quenched with 20 mL of saturated aqueous sodium sulfate, diluted with 200 mL of diethyl ether, and then allowed to warm to room temperature with vigorous stirring. The pH of the

(19) Bharadwaj, P. K.; Potenza, J. A.; Schugar, H. J. *Acta Crystallogr.* **1988**, *C44*, 763−5.

(20) (a) Bharadwaj, P. K.; Fikar, R.; Potenza, M. N.; Zhang, X.; Potenza, J. A.; Schugar, H. J. Unpublished results. (b) Fox, S.; Potenza, J. A.; Knapp, S.; Schugar, H. J. Unpublished results.

Table 1. Crystallographic Data for Ligand **9** and for Metal Complexes with the Bis(disulfide) Ligands **9** and **16**

	meso-**9**·H_2O	*rac*-**9**	**17**·2CH_3CN	*meso*-**10**	*meso*-**8**	*meso*-**7**
formula	$S_4ON_4C_{28}H_{58}$	$S_4N_4C_{28}H_{56}$	$Cu_2S_4O_4N_{10}C_{34}H_{62}$	$Cu_2S_4O_4N_8C_{32}H_{56}$	$I_4Cu_2S_4N_6C_{32}H_{62}$	$I_4Ni_2S_4N_6C_{32}H_{62}$
fw	595.06	577.01	930.27	872.2	1293.84	1284.18
a, Å	26.310(2)	12.031(2)	11.846(1)	7.909(2)	10.085(2)	10.119(3)
b, Å	11.420(5)	9.706(2)	15.576(2)	20.572(3)	12.325(2)	12.288(4)
c, Å	11.988(1)	28.769(3)	12.803(1)	12.263(2)	10.091(2)	10.121(3)
α, deg					104.81(3)	104.68(2)
β, deg	106.259(7)	93.07(1)	102.32(2)	92.08(1)	98.72(3)	98.39(2)
γ, deg					104.59(3)	104.75(2)
V, Å^3	3458(2)	3354.7(8)	2307.8(8)	1994(1)	1141.7(4)	2295.9(6)
space group	*C*2/*c*	*P*2$_1$/*c*	*P*2$_1$/*c*	*P*2$_1$/*c*	*P*1	*P*1
Z	4	4	2	2	1	1
ρ_{calcd}, g/cm^3	1.143	1.142	1.339	1.453	1.882	1.857
ρ_{obs}, g/cm^3	1.12(1)		1.34(1)	1.40(1)	1.85(1)	1.85(1)
μ, cm^{-1}	2.9	2.8	11.4	13.1	38.6	37.2
trans factor range	0.97−1.00	0.49−0.77	0.97−1.00	0.98−1.00	0.46−0.99	0.78−0.99
temp, K	296(1)	293(2)	296(1)	298(1)	298(1)	299(1)
no. of data used in refinement	2086	4291	1888	1509	3384	1259
selection criterion	$I > 3\sigma(I)$	all F_o^2	$I > 2\sigma(I)$	$I > 3\sigma(I)$	all data	$I > 2\sigma(I)$
R_F,[a] R_{wF}[b] (R_{wF}^2)[c]	0.033, 0.049	0.059, (0.159)	0.034, 0.040	0.041, 0.048	0.077, (0.202)	0.032, 0.093
selection criteria for R_F;[a] R_{wF}[b] (R_{wF}^2)[c]	$I > 3\sigma(I)$; $I > 3\sigma(I)$	$I > 2\sigma(I)$; all data	$I > 2\sigma(I)$; $I > 2\sigma(I)$	$I > 3\sigma(I)$; $I > 3\sigma(I)$	$I > 2\sigma(I)$; all data	$I > 2\sigma(I)$; all data

[a] $R_F = \sum||F_o| - |F_c||/\sum|F_o|$. [b] $R_{wF} = [\sum w(|F_o| - |F_c|)^2/\sum wF_o^2]^{1/2}$. [c] $R_{wF}^2 = [\sum[w(F_o^2 - F_c^2)^2]/\sum[w(F_o^2)^2]]^{1/2}$.

resulting paste was lowered to ∼9 by the addition of approximately 40 mL of 1 M aqueous HCl. The resulting white precipitate was removed by filtration, and the filtrate was washed with water (2 × 400 mL), dried over anhydrous $MgSO_4$, and then concentrated to afford 12.84 g (91%) of ligand **13** as a pale yellow oil: ^{13}C NMR (100 MHz) 64.46 (*C*H$_2$−NH), 60.00 (*C*H−NH), 45.78 (4° *C*−SH), 35.62 (4° *C*−CH$_2$NH), 30.50 (*C*H$_3$−C−SH), 24.74 (*C*H$_3$−C); ^{1}H NMR (400 MHz) 2.58 (s, 4 H), 2.51 (s, 4 H), 1.75 (br s, 4 H), 1.35 (s, 12 H), 0.94 (s, 6 H).

***N,N′*-Bis-(2-methyl-2-mercapto-prop-1-yl)-1,3-diamino-2,2-dimethyl-propanenickel(II) (14).** A filtered solution containing 0.750 g (2.92 mmol) of Ni(acac)$_2$ in 25 mL of dichloromethane was added to a solution of 1.11 g (4.0 mmol) of **13** in 25 mL of dichloromethane. The resulting clear brown solution was concentrated to a sparkling brown paste. Removal of the acetylacetone was accomplished by the addition of 25 mL of ether. Complex **14** separated as a brown powder, which was collected by filtration, washed with 25 mL of ether, and dried in air to afford 0.98 g (98%) of crude product. Crude **14** was recrystallized as light red needles by slow evaporation from acetone/isooctane mixtures and has been characterized structurally and spectroscopically; complete details will be reported elsewhere.[20b]

[Ni(16)I$_2$(CH$_3$CN)$_2$]$^{2+}$2I$^-$ (15). A solution of 1.016 g (4 mmol) of iodine in 50 mL of acetonitrile was added to a solution of 1.34 g (4 mmol) of crude **14** in 25 mL of acetonitrile to afford a deep-red solution that was filtered and allowed to stand. After 3 days, a crop of sparkling yellow-green crystals was collected by decantation and dried in air to afford 1.025 g (40%) of complex **15**.

3,3,7,7,11,11,14,14,18,18,22,22-Dodecamethyl-5,9,16,20-tetraaza-1,2,12,13-tetrathia-cyclododecosane (16). A mixture of 0.400 g (0.317 mmol) of **15** (ground to a yellow powder), 150 mL of water, and 15 mL of acetonitrile was stirred at room temperature. The resulting white fluffy precipitate was collected by filtration and dried in vacuo to give 0.12 g (68%) of free ligand **16**: ^{1}H NMR (400 MHz) 2.57 (s, 4 H), 2.44 (s, 4 H), 1.50 (br s, 4 H), 1.28 (s, 12 H), 0.89 (s, 6 H). Anal. Calcd (Found) for $S_4N_4C_{26}H_{56}$: S, 23.19 (23.06); N, 10.13 (10.14); C, 56.47 (56.38); H, 10.21 (10.08).

Cu$_2$(16)(NCO)$_4$·2CH$_3$CN (17). A sky-blue paste was prepared by dissolving 0.016 g (0.2 mmol) of potassium cyanate in 2 drops of water and adding 0.037 g (0.1 mmol) of Cu(ClO$_4$)$_2$·6H$_2$O. The paste was dissolved in 5 mL of acetonitrile and immediately filtered into a filtered solution of 0.030 g (0.054 mmol) of **16** in 10 mL of acetonitrile. The resulting yellow-green solution was stirred vigorously for 15 min, and the product was collected by filtration, washed with 10 mL of acetonitrile, and then dried in vacuo to afford 0.017 g (33% based upon **16**) of yellow-green crystalline **17**. Diffraction-quality crystals were obtained by recrystallization from acetonitrile.

X-ray Crystallography. (a) General Procedures. An Enraf-Nonius CAD-4 diffractometer was used for data collection. Graphite-monochromated Mo Kα radiation (λ = 0.710 73 Å) was used for all structures except *rac*-**9,** for which graphite-monochromated Cu Kα radiation (λ = 1.541 84 Å) was used. The Enraf-Nonius Structure Determination Package[21a] was used for data collection for all structures and for the processing of data, structure solution, and refinement of *meso*-**9**, *meso*-**10**, and **17**. Data for *rac*-**9**, *meso*-**7**, and *meso*-**8** were processed, and the structures were solved and refined using the SHELX system.[21b,c] Lattice dimensions and Laue symmetry were checked for all crystals by using axial photographs. Systematic searches for higher symmetry cells were conducted using the program TRACER. Data were collected using $\theta-2\theta$ scans with scan ranges given by $a + b \tan\theta$, where a = 0.60 or 0.8° and b = 0.35°. Crystal data and additional details of the data collection and refinement for the six crystals studied are given in Table 1 and as Supporting Information. For each crystal, intensity data were corrected for decay, absorption (empirical, ψ scan), and Lorentz−polarization effects. Partial structures were obtained by direct methods, and the remaining non-hydrogen atoms in each structure were located by using difference Fourier techniques. H atoms were located on difference Fourier maps or placed at calculated positions. For H atoms whose thermal parameters were not refined, isotropic temperature factors were set equal to (1.2−1.5)U_N, where N is the atom bonded to H. All structures were refined by using full-matrix least-squares techniques. Refinements for *rac*-**9**, *meso*-**7**, and *meso*-**8** were based on F^2; those for the remaining structures were based on F. Views of the structures were prepared by using ORTEP3 for Windows.[22] Crystallographic details for the individual structures follow. Additional details are available as Supporting Information.

(b) *meso*-9·H$_2$O. A white crystal measuring 0.12 × 0.16 × 0.17 mm was mounted on the end of a glass fiber. All H atoms except those for the water molecule were located and refined isotropically. The water oxygen atom was located approximately 1 Å from a 2-fold axis (O···O′ = 1.97(1) Å), suggesting partial occupancy. An occupancy factor of 0.5 was determined by variation of the site occupancy factor.

(21) (a) *Enraf-Nonius Structure Determination Package*; Enraf-Nonius: Delft, Holland, 1983. (b) Sheldrick, G. M. SHELXS-97. *Acta Crystallogr.* **1990**, *A46*, 467−73. (c) Sheldrick, G. M. *SHELXL-97*: *A computer Program for Refinement of Crystal Structures*; University of Göttingen: Germany.

(22) Farrugia, L. J. *ORTEP3 for Windows*, version 1.0.5; University of Glasgow: Scotland, 1997.

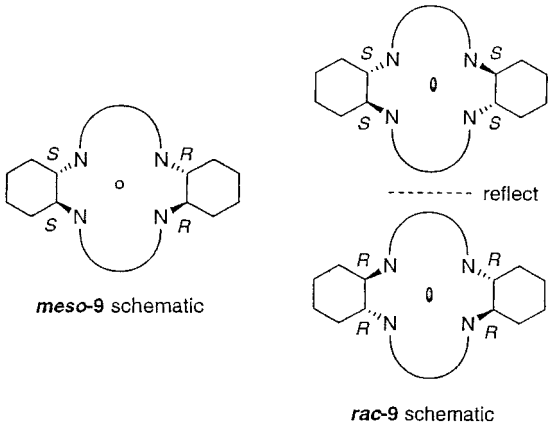

Figure 1. Sketch showing the relationship of the cyclohexane−N_2S_2 units for *meso*-**9** and the diastereomers of *rac*-**9**.

Ligand *meso*-**9** utilizes a crystallographic center of symmetry at $^3/_4$, $^1/_4$, 0 (4*d* site symmetry in *C*2/*c*) and therefore is the meso isomer of macrocycle **9**. Meso and racemic forms of **9** are sketched in Figure 1.

(c) *rac*-9. A colorless crystal measuring 0.10 × 0.22 × 0.30 mm was mounted on the end of a glass fiber. H atoms were located and refined isotropically. Macrocycle *rac*-**9** crystallizes in the centrosymmetric space group $P2_1/c$ with four molecules in general positions. Examination of the structure revealed that it is the racemate containing centrosymmetrically related enantiomers.

(d) Cu_2(16)$(NCO)_4$·2CH_3CN (17). A yellow-green crystal measuring 0.12 × 0.14 × 0.21 mm was coated with a thin film of epoxy cement and mounted on the end of a glass fiber. Solution of the structure revealed two solvate molecules of acetonitrile per molecule of Cu_2(**16**)$(NCO)_4$. The Cu_2(**16**)$(NCO)_4$ molecule utilizes a crystallographic center of symmetry at 0, 0, $^1/_2$ (2*c* site symmetry in $P2_1/c$). All H atoms were located, and their coordinates were refined.

(e) Cu_2(*meso*-9)$(NCO)_4$ (*meso*-10). A green crystal measuring 0.10 × 0.16 × 0.17 mm was mounted at the end of a glass fiber. H atoms were located on a difference Fourier map or placed at calculated positions and were not refined. The Cu_2(*meso*-**9**)$(NCO)_4$ molecule utilizes a crystallographic center of symmetry at $^1/_2$, 0, $^1/_2$ (2*d* site symmetry in $P2_1/c$), requiring it to be the meso isomer.

(f) $[Cu_2$(*meso*-9)(2I)$(CH_3CN)_2]^{2+}$ $2I^-$ (*meso*-8). A black crystal (0.06 × 0.13 × 0.23 mm) was mounted at the end of a glass rod. Some difficulty was encountered in solving the structure, as outlined below. Examination of the reciprocal lattice revealed a triclinic system containing one cation and two anions in a unit cell for which $a = c$ and $\alpha = \gamma$ to within experimental error. This triclinic cell was transformed to a *C*-centered monoclinic cell also with no systematic absences, consistent with space groups *C*2, *Cm*, or *C*2/*m*, each with two cations per cell. Solutions were examined in the five possible space groups (*P*1, $P\bar{1}$, *C*2, *Cm*, and *C*2/*m*). Of these, only *P*1 and $P\bar{1}$ are consistent with cations having cyclohexane rings in the expected chair conformation. In $P\bar{1}$, the cations must utilize a crystallographic center of symmetry similar to those of the macrocycles in *meso*-**9** and *meso*-**10**. As with the monoclinic space groups, in which the cation must show 2, *m*, or 2/*m* point symmetry, refinement in $P\bar{1}$ led to planar cyclohexane rings and disordered five-membered NS-chelate rings. The best fit to the data was obtained in space group *P*1 with 38 soft distance restraints applied to bonds among the atoms in the four unique NS-chelate rings and two unique cyclohexane rings. All non-hydrogen atoms were refined anisotropically; H atoms were added to the structure at calculated positions and were not refined. Refinement resulted in the expected chair conformation of the cyclohexane rings and in chelate rings, although both types of rings exhibited some disorder. The eight unique methyl groups showed relatively large thermal parameters; two were considered disordered and were modeled by using two half-occupied sites. Although there is some possibility that the crystal is twinned, this is not indicated by the Flack parameter, which refined to 0.10(5). Our interest in this structure and that of *meso*-**7**, discussed below, lies in their coordination geometries. In both structures, atoms in the coordination spheres exhibit approximate 2/*m* point symmetry, are relatively insensitive to refinement, and show little if any sign of disorder in the several possible space groups. For these reasons, we did not pursue twinning further and have reported the structures of *meso*-**8** and *meso*-**7** in space group *P*1.

At first glance, the disorder of the cyclohexane and chelate ring atoms appears consistent with a structure containing a mixture of all three isomers of **9**. Such a mixture could arise from the method of preparation of **8** directly from the oxidative coupling reaction of *rac*-**6** (Scheme 1). Evidence for isolation of the meso isomer of **8**, in which the cations cannot utilize either a crystallographic 2-fold axis or a mirror plane without introducing substantial disorder, and further justification of the choice of space group are presented in the discussion section below.

(g) $[Ni_2$(*meso*-9)(2I)$(CH_3CN)_2]^{2+}$ $2I^-$ (*meso*-7). Difficulty was encountered in obtaining crystals of **7** with peak profiles suitable for X-ray diffraction studies. Approximately 20 crystals from several batches were examined, and two data sets were collected. The structure reported is from a green crystal of dimensions 0.06 × 0.20 × 0.20 mm that was mounted in a glass capillary with a small amount of acetonitrile well removed from the crystal. The structure of *meso*-**7** is isomorphous with that of *meso*-**8**, and consequently similar difficulties were encountered in solving the structure. As with *meso*-**8**, structure solutions were examined in space groups *P*1, $P\bar{1}$, *C*2, *Cm*, and *C*2/*m* with similar results. We report the refined structure in space group *P*1. All non-hydrogen atoms were refined anisotropically; H atoms were added to the structure at calculated positions and were not refined.

Results and Discussion

Description of the Structures. Views of *meso*-**9**·H_2O, *rac*-**9**, **17**, *meso*-**10**, and *meso*-**8**, showing the crystallographic numbering schemes, are given in Figure 2. Metric data for several structures are listed in Table 2.

The structure of *meso*-**9**·H_2O consists of centrosymmetric *meso*-heteroeicosane macrocycles separated by water solvate molecules. There are no unusually short intermolecular contacts. When viewed in profile, approximately normal to the S−S bonds (Figure 3a), the molecule is seen to have a stepped or kinked conformation with the two approximately planar elaborated cyclohexane halves corresponding to the run and the disulfide groups to the rise. This structural motif is maintained in the metal complexes *meso*-**7**, *meso*-**8**, *meso*-**10**, and **17** (Figure 3). Ligand *rac*-**9** is a racemic mixture of centrosymmetrically related macrocycles; in contrast to *meso*-**9**, *rac*-**9** appears V-shaped in profile with the disulfide groups near the vertex of the V (Figure 3b). Ligand **18**[23a] provides a structurally characterized example of a 20-membered ring with the same ring connectivity as that of **9**. In contrast to *meso*-**9** and *rac*-**9**, **18** adopts a cage conformation with two of the benzo substituents forming the base of the cage.

In both *meso*-**9** and *rac*-**9**, the cyclohexane rings show no signs of disorder; they exhibit the chair conformation as expected, and their metric parameters are typical (average C−C bond distances of 1.520(8) and 1.518(24) Å and average interior angles of 111.4(8) and 111.6(11)° for *meso*-**9** and *rac*-**9**, respectively).

A comparison of the metric parameters of the disulfide groups in *meso*-**9** and *rac*-**9** (Table 2) with those in the structurally similar compounds *rac*-**3**,[19] **19**,[24] **20**,[24] and **21**[24] reveals little variation in the S−S distances (range of 2.020(1)−2.043(2) Å), the S−C distances (range of 1.845(4)−1.869(2) Å), and the S−S−C angles (range of 105.5(1)−109.79(5) Å). Compound **18**,[23a] with S atoms bonded directly to benzo groups, exhibits a

(23) (a) Tsagkalidis, W.; Rodewald, D.; Rehder, D. *Inorg. Chem.* **1995**, *34*, 1943−5. (b) Jørgensen, F. S.; Snyder, J. P. *J. Org. Chem.* **1980**, *45*, 1015−20.

(24) Jackson, T. W.; Kojima, M.; Lambrecht, R. M.; Marubayashi, N.; Hiratake, M. *Aust. J. Chem.* **1994**, *47*, 2271−7.

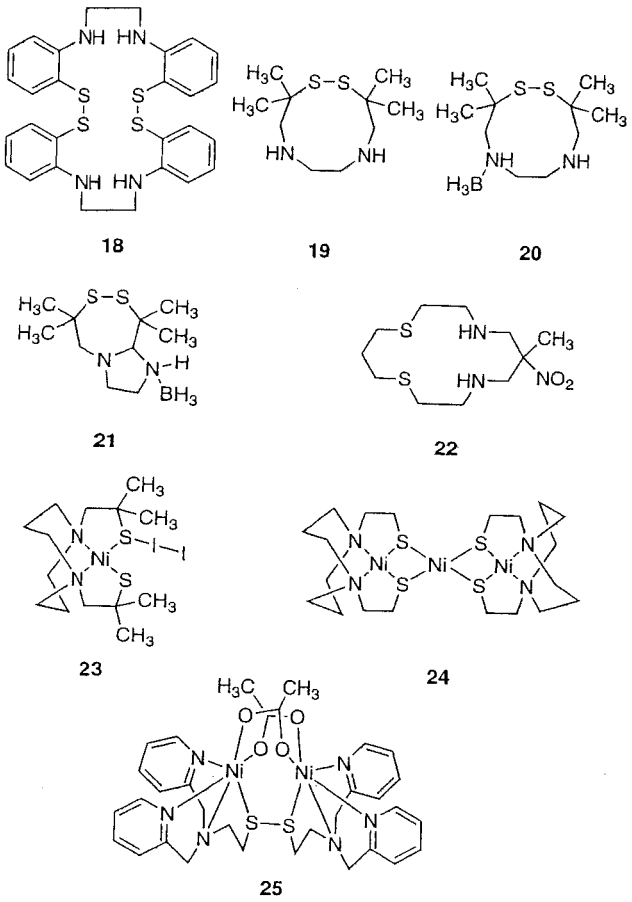

longer S−S distance (2.0829(7) Å) and shorter S−C distances (1.764(2) and 1.772(2) Å). Larger variations are observed for the C−S−S−C dihedral angles, which range from 90.8(1)° in *rac*-**3** (close to the "natural" disulfide dihedral angle for strain-free disulfides[23b]) to 125.5(2)° in **21**.

The structure of **17**·2CH_3CN consists of discrete centrosymmetric bimetalated molecules of the heterodocosane ligand **16** separated by acetonitrile molecules of solvation. There are no unusually short intermolecular contacts. Complex **17** exhibits a Cu coordination geometry that is best described as axially compressed distorted cis-octahedral with the axis of compression approximately parallel to the N3−N4 vector. The Cu−N(amine) distances (2.147(4) and 2.150(4) Å, Table 2) perpendicular to the compression axis are significantly *longer* than those reported for the corresponding Cu−N(amine) equatorial bonds in *meso*-**8**, *meso*-**10**, and **22** (2.017(6) and 2.030(5) Å),[25] whereas the Cu−N(NCO) bond lengths (1.894(4) and 1.884(4) Å) are at the *short* end of the range (1.889(3)−1.955(7) Å) observed for Cu−N(NCO) equatorial bonds in a variety of bis(isocyanato) copper(II) complexes.[26−30] A substantially longer Cu−(NCO) bond length (2.188(7) Å) has been observed[28] for an axially bound isocyanate ligand in a Cu(II) complex with square-pyramidal coordination.

Cu(II)−S(disulfide) linkages are relatively rare; several that have been reported are for axial linkages of either square-pyramidal (2.798(1);[8] 2.678(2);[5] 3.16(1) and 3.28(1) Å[7]) or tetragonal (3.057(10) and 3.138(9) Å[6]) complexes. Axial Cu(II)−S(thioether) linkages as long as 3.001(2) Å have also been reported.[31] In **17**, the equatorial Cu−S distances (2.929(1) and 3.097(1) Å) fall within the range of 2.721−3.28 Å for axial Cu(II)−S(disulfide) linkages noted above, yet are substantially longer than typical Cu(II)−S(equatorial) bonds.[32] To what extent do the Cu−S interactions in **17** constitute bonding? Using SCF-Xα-SW calculations, Lowery and Solomon[33] have determined that the methionine group in poplar plastocyanin, for which a Cu(II)−S(methionine) distance of 2.90 Å has been determined crystallographically,[34] binds covalently to Cu(II) with a bond strength of approximately 30%. Cu(II)−S(methionine) distances in several other copper-containing proteins, ranging from 2.61 Å in cucumber basic protein to 3.16 Å in azurin, have been reported,[35a] and even the relatively long linkage in azurin is thought to represent some covalent bonding.[35b] Moreover, bond angles at Cu for **17** (Table 2), including those involving the disulfide S atoms, show an average deviation from ideal octahedral values of approximately 7° and lend support for a distorted cis-octahedral interpretation of the coordination geometry. The macrocyclic ligand **16** is expected to be flexible in the vicinity of the disulfide groups, and there would appear to be no steric reason the S atoms could not be located further from Cu as in *meso*-**10**, for which one Cu···S distance is >4 Å. Taken together, these data suggest that there are weak Cu−S bonding interactions in **17**. Given the discussion above, the coordination geometry in **17** can be described either as axially compressed distorted cis-octahedral or as a four-coordinate seesaw arrangement with two additional semicoordinated S(disulfide) ligands. Axially compressed six-coordinate Cu(II) complexes with two short and four long bonds are known, and their geometries have been understood to result from pseudo-Jahn−Teller effects.[36]

In *meso*-**10**, the ligand exhibits the stepped conformation in profile and a center of symmetry coinciding with the center of mass of the molecule, both of which are characteristic of the meso conformation. The copper coordination geometry is best described as trigonal-bipyramidal CuN_4S, with one amine nitrogen atom (N1) and one isocyanate nitrogen atom (N4) apical. The Cu−S bond in *meso*-**10** provides a rare example of an equatorial Cu(II)−S(disulfide) linkage. Its length (2.505(2) Å) falls within the range reported (2.33−2.56 Å)[32] for several equatorial Cu(II)−S(thioether) linkages in trigonal-bipyramidal CuN_4S(thioether) complexes. The nonbonding sulfur atom S2 is situated 4.015(2) Å from Cu and is too far away to be considered bonded. However, S2′, which is bonded to the sulfur bonded to Cu, is located 3.253(2) Å from Cu, possibly suggesting some dihapto character for the bonding disulfide ligand. Compression of the trigonal bipyramid along its pseudo-3-fold axis is suggested by a consideration of the Cu−N(amine) and Cu−N(isocyanate) distances; in each case, the axial bond is ca. 0.1 Å shorter than the corresponding equatorial bond.

(25) Comba, P.; Lawrance, G. A.; Rossignoli, M.; Skelton, B. W.; White, A. H. *Aust. J. Chem.* **1988**, *41*, 773−81.
(26) Pickardt, J.; Rautenberg, N. *Z. Naturforsch., B* **1982**, *37*, 1569−72.
(27) Valach, F.; Dunaj-Jurèo, M. *Acta Crystallogr.* **1982**, *B38*, 2145−8.
(28) Rojo, T.; Garcia, A.; Mesa, J. L.; Arriortua, M. I.; Pizarro, J. L.; Fuertes, A. *Polyhedron* **1989**, *8*, 97−102.
(29) Otieno, T.; Rettig, S. J.; Thompson, R. C.; Trotter, J. *Inorg. Chem.* **1993**, *32*, 4384−90.
(30) Kabesŏvá, M.; Jorík, V.; Dunaj-Jurćo, M. *Acta Crystallogr.* **1993**, *C49*, 1120−1.
(31) Juen, S.; Xueyi, L.; Liaorong, C.; Baoshen, L. *Inorg. Chim. Acta* **1988**, *153*, 5−7.
(32) Bouwman, E.; Driessen, W. L.; Reedijk, J. *Coord. Chem. Rev.* **1990**, *104*, 143−72.
(33) Lowery, M. D.; Solomon, E. I. *Inorg. Chim. Acta* **1992**, *198−200*, 233−43.
(34) (a) Guss, J. M.; Freeman, H. C. *J. Mol. Biol.* **1983**, *169*, 512−63. (b) Guss, J. M.; Harrowell, P. R.; Murata, M.; Norris, V. A.; Freeman, H. C. *J. Mol. Biol.* **1986**, *192*, 361−87.
(35) (a) Guss, J. M.; Merritt, E. A.; Phizackerley, R. P.; Freeman, H. C. *J. Mol. Biol.* **1996**, *262*, 686−705. (b) Solomon, E. I.; Baldwin, M. J.; Lowery, M. D. *Chem. Rev.* **1992**, *92*, 521−42.
(36) Hathaway, B. J. *Struct. Bonding* **1984**, *57*, 55−118.

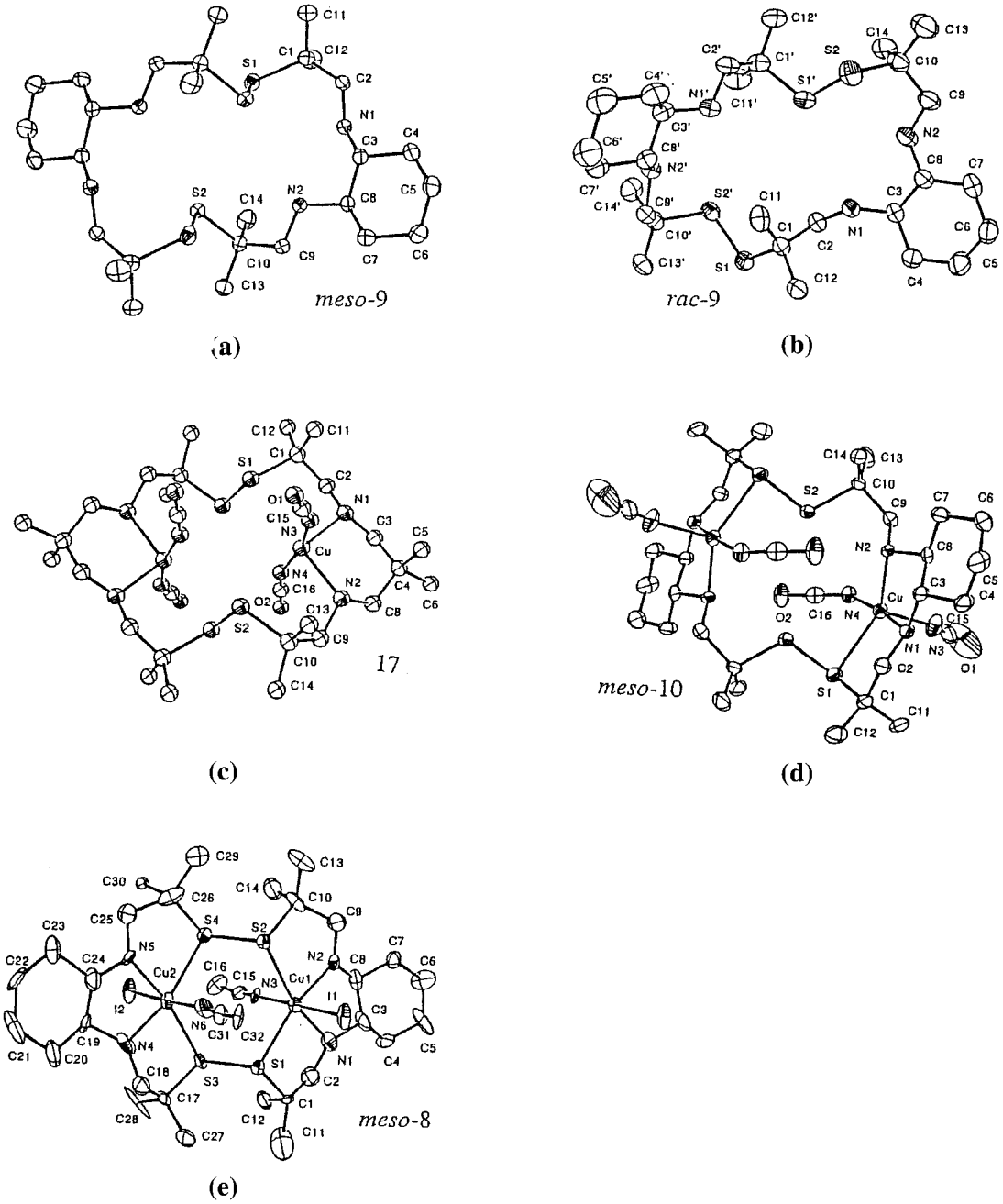

Figure 2. Views of (a) *meso*-**9**, (b) *rac*-**9**, (c) **17**, (d) *meso*-**10**, and (e) *meso*-**8**, showing the atom numbering schemes. *meso*-**7** is isostructural with *meso*-**8** and has the same numbering scheme. Anions, molecules of solvation, and hydrogen atoms have been omitted for clarity.

In principle, oxidative coupling of *rac*-**5** or *rac*-**6** (Scheme 1) could lead to a mixture of meso and racemic isomers of **7** and/or **8**. Crystals isolated from the coupling reactions contain only the meso isomers based on the conformation of the cations. In both *meso*-**7** and *meso*-**8**, the cations exhibit the step conformation in profile (Figure 3c) characteristic of *meso*-**9**, with no evidence of the V-shaped conformation (Figure 3b) corresponding to *rac*-**9**. Indeed, all of the metal-containing complexes of **9** that we have characterized crystallographically show the ligand in the step conformation, consistent with the meso isomer, possibly because axial ligation would lead to crowding in the vicinity of the vertex of the V (Figure 3b). Macrocycle **9** precipitates as a crystalline mixture of *meso*-**9** and *rac*-**9** following demetalation of *meso*-**7**, suggesting the possibility of disulfide scrambling during the demetalation process.

Crystals of *meso*-**8** and its isomorphous analogue *meso*-**7** show the step conformation characteristic of meso complexes, yet in contrast to *meso*-**9**, *meso*-**10**, and **17**, they exhibit thermal and positional parameters consistent with some disorder of the chelate and cyclohexane rings. Of the five possible space groups for *meso*-**7** and *meso*-**8**, refinement in *C*2 introduced a 2-fold axis passing through the midpoints of the S−S bonds, refinement in *Cm* resulted in a mirror plane containing the axial ligands and the metal atoms, and refinement in *C*2/*m* gave rise to both of these symmetry elements. In each case, the result was flattening of the chelate and cyclohexane rings, presumably as a consequence of the site symmetry imposed. Of the remaining two possible space groups, refinement in $P\bar{1}$, with the center of symmetry at the center of mass of the cation, resulted in chelate rings that exhibited substantially greater disorder than those obtained from refinement in space group *P*1. An examination of the five-membered NS-chelate rings in *P*1 shows that they all have the envelope conformation with each methylene carbon atom (C2, C9, C18, and C25) corresponding to a flap. The

Table 2. Metric Parameters for Ligand **9** and for Metal Complexes with Ligands **9** and **16** (Distances Are in Angstroms and Angles Are in Degrees)

	meso-**9**·H_2O	*rac*-**9**	**17**·2CH_3CN	*meso*-**10**	*meso*-**8**	*meso*-**7**
M−N1			2.147(4)	2.032(5)	2.022(3)	1.954(9)
M−N2			2.150(4)	2.118(5)	2.053(3)	2.03(1)
M−N3			1.894(4)	2.064(7)	2.037(3)	2.15(1)
M−N4			1.884(4)	1.928(6)	2.032(3)	2.12(1)
M−N5					2.047(3)	2.18(1)
M−N6					2.082(5)	1.98(2)
M−S1			2.929(1)	2.505(2)	2.504(1)	2.519(4)
M−S2			3.097(1)	4.015(2)	2.522(1)	2.565(4)
M−S2′				3.253(2)		
M−S3					2.539(1)	2.456(5)
M−S4					2.547(2)	2.509(5)
M−I1					2.7676(7)	2.796(3)
M−I2					2.7734(7)	2.762(3)
S1−S2′(S3)	2.0368(8)	2.030(1)	2.035(1)	2.044(3)	2.047(1)	2.015(6)
S2−S1′(S4)		2.030(2)			2.074(1)	2.108(6)
S1−C1, S1′-C1′	1.859(2)	1.850(3), 1.862(4)	1.863(5)	1.850(7)	1.879(3)	1.90(1)
S3−C17					1.857(4)	1.85(1)
S2−C10, S2′−C10′	1.856(2)	1.851(4), 1.862(3)	1.857(5)	1.869(7)	1.905(4)	1.87(1)
S4−C26					1.897(4)	1.88(1)
C1−C2, C1′-C2′	1.516(3)	1.524(4), 1.506(6)	1.520(7)	1.52(1)	1.484(5)	1.50(1)
C17−C18					1.499(5)	1.52(1)
C9−C10, C9′-C10′	1.524(3)	1.546(6), 1.522(5)	1.513(7)	1.531(9)	1.510(5)	1.51(1)
C25−C26					1.517(5)	1.48(1)
N1−C2, N1′-C2′	1.463(3)	1.457(4), 1.456(5)	1.475(6)	1.494(9)	1.439(5)	1.47(1)
N4−C18					1.431(5)	1.47(1)
N2−C9, N2′-C9′	1.455(3)	1.440(5), 1.463(4)	1.468(6)	1.483(9)	1.443(5)	1.43(1)
N5−C25					1.463(5)	1.42(1)
M···M′			4.573(1)	5.813(2)	4.2196(7)	4.220(3)
C1−S1−S2′-C10′	109.50(9)	110.1(2), 112.6(2)	106.0(2)	108.5(3)		
C17−S3−S1−C1					94.6(2)	92.1(7)
C10−S2−S1′-C1′						
C10−S2−S4−C26					90.7(2)	90.7(6)

	17· 2CH_3CN	*meso*-**10**	*meso*-**8**	*meso*-**7**
S1−M−S2, S3−M−S4	106.70(3)		110.64(4), 110.95(4)	110.2(1), 110.7(2)
S1−M−N1, S3−M−N4	78.4(1)	83.9(2)	84.1(1), 83.6(1)	83.8(3), 83.0(3)
S1−M−N2, S3−M−N5	177.1(1)	139.0(2)	167.3(1), 167.8(1)	167.2(2), 167.4(3)
S2−M−N1, S4−M−N4	174.8(1)		165.2(1), 165.4(1)	164.8(3), 166.1(3)
S2−M−N2, S4−M−N5	75.8(1)		81.6(1), 81.0(1)	81.3(3), 81.2(3)
S1−M−N3, S4−M−N6	86.5(1)	110.5(2)	91.1(1), 91.4(1)	91.7(4), 91.4(5)
S2−M−N3, S3−M−N6	85.5(1)		89.6(1), 93.0(1)	93.0(3), 89.5(5)
S1−M−N4, S2−M−N4	86.6(1), 85.6(1)	90.0(2)		
S1−M−I, S4−M−I			85.58(3), 84.69(4)	85.2(2), 84.3(1)
S2−M−I, S3−M−I			85.45(3), 84.77(3)	84.1(1), 86.1(2)
N1−M−N2, N4−M−N5	99.0(2)	83.5(2)	83.6(1), 84.4(1)	84.3(4), 85.0(4)
N1−M−N3, N5−M−N6	95.4(2)	87.5(3)	92.0(1), 89.1(1)	92.7(4), 86.0(6)
N2−M−N3, N4−M−N6	95.2(2)	107.1(3)	92.3(1), 89.4(2)	93.2(5), 86.4(6)
N1−M−I, N5−M−I			94.1(1), 94.1(1)	91.2(3), 99.6(4)
N2−M−I, N4−M−I			92.4(1), 95.4(1)	90.7(4), 99.2(4)
N3−M−I, N6−M−I			172.60(8), 174.5(1)	174.7(2), 172.3(4)
N1−M−N4	94.4(2)	171.3(2)		
N2−M−N4	92.2(1)	97.3(2)		
N3−M−N4	166.7(2)	100.4(2)		

arrangement of the four unique flaps is inconsistent with a center of symmetry, favoring $P1$ over $P\bar{1}$ as the more likely space group, but this subtle difference may be an artifact of the refinement process. As noted above, the coordination geometries are relatively insensitive to the choice of space group and we restrict our comments below to them. Both *meso*-**7** and *meso*-**8** exhibit distorted-octahedral MN_3S_2I coordination. In each instance, *meso*-**9** acts as an octadentate ligand, forming four equatorial bonds to each metal ion, two cis M−S(disulfide) and two cis M−N(amine). Coordination is completed by trans M−I and M−N(nitrile) linkages.

In *meso*-**8**, the Cu−S(disulfide) bonds are, within ±0.02 Å, equal in length to the equatorial Cu(II)−S(disulfide) linkage in trigonal-bipyramidal *meso*-**10** and constitute strong bonding interactions (vide supra). The Cu−N(nitrile) distances (2.037(3) and 2.082(5) Å) lie near the short end of the range reported for equatorial (1.984(3) Å[37]) and axial (2.491(6),[38] 2.526(8),[39] and 2.570(5)[40] Å) Cu(II)−N($NCCH_3$) bonds in six-coordinate copper(II) complexes. Thus, their lengths are consistent with equatorial bonding. The six-coordinate Cu(II) complex Cu(II)-(imidazole)$_4I_2$ contains *axial* iodide ions with Cu−I distances of 3.42 and 3.87 Å,[41] much longer than the Cu−I distances in

(37) Blake, A. J.; Fallis, I. A.; Gould, R. O.; Parsons, S.; Ross, S. A.; Schröder, M. *J. Chem. Soc., Chem. Commun*. **1994**, 2467−9.
(38) Oshio, H. *Inorg. Chem*. **1993**, *32*, 4123−30.
(39) Dedert, P. L.; Thompson, J. S.; Ibers, J. A.; Marks, T. J. *Inorg. Chem*. **1982**, *21*, 969−77.
(40) Scott, M. J.; Holm, R. H. *J. Am. Chem. Soc*. **1994**, *116*, 11357−67.
(41) Akhtar, F.; Goodgame, D. M. L.; Goodgame, M.; Rayner-Canham, G. W.; Skapski, A. C. *J. Chem. Soc., Chem. Commun*. **1968**, 1389−90.

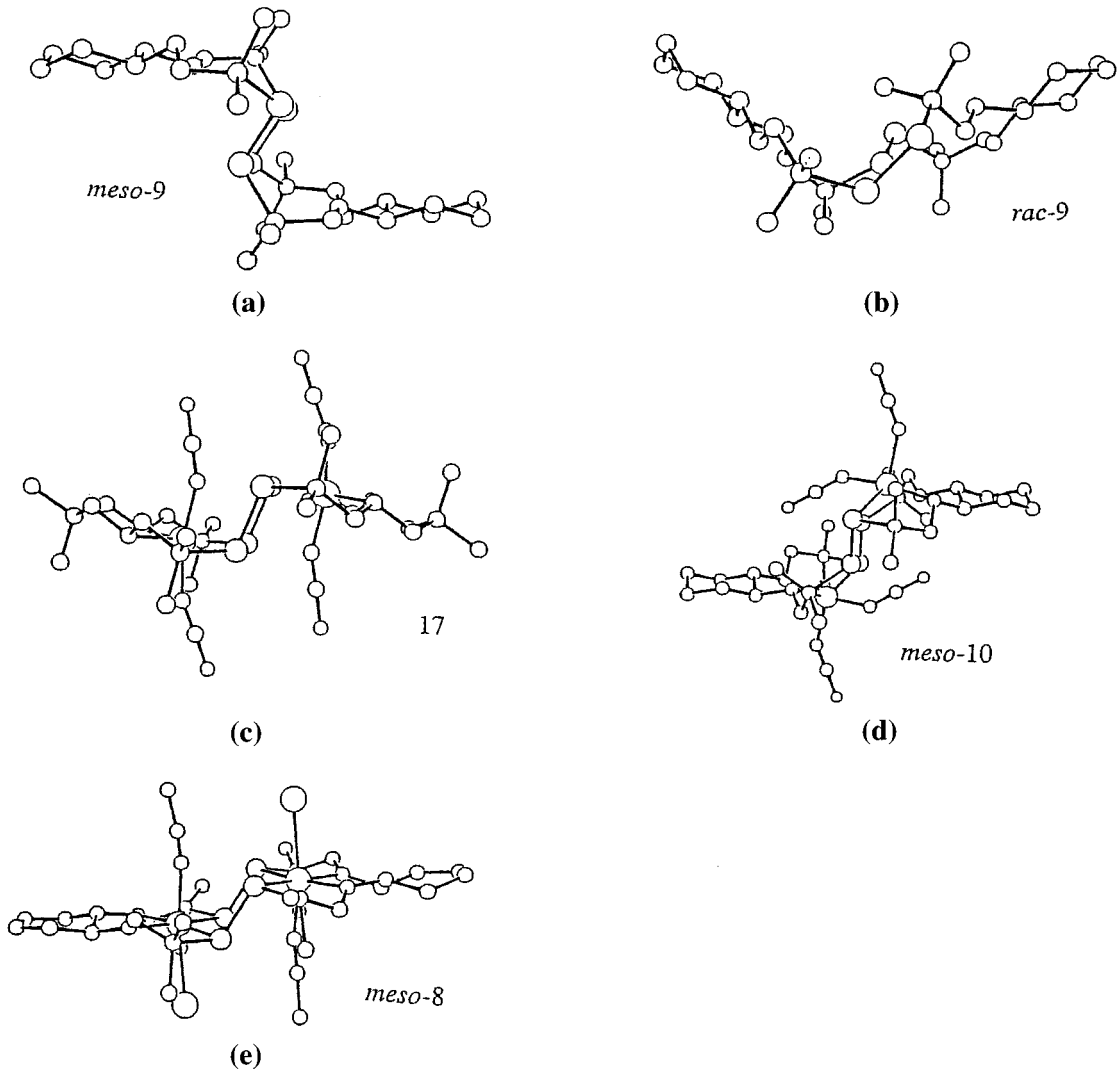

Figure 3. Edge-on PLUTO views of (a) *meso*-**9**, (b) *rac*-**9**, (c) **17**, (d) *meso*-**10**, and (e) *meso*-**8** showing the conformational differences of the several ligands and metal complexes. Note the difference in shape of the ligands *meso*-**9** and *rac*-**9**. Anions, molecules of solvation, and hydrogen atoms have been omitted for clarity.

meso-**8** (2.7676(7) and 2.7734(7) Å), which lie within the range (2.6454(9)−2.806(2) Å) observed[42−45] for Cu(II)−I distances in a variety of five-coordinate trigonal-bipyramidal and square-pyramidal complexes. In sum, the coordination geometry in *meso*-**8** is unusual in that Cu(II) appears to form *six* full-strength bonds in a distorted octahedral environment. We are aware of no other Cu(II) complex in which this situation obtains.

In *meso*-**7**, bond distances are all typical for their types. Thus, the Ni−S(disulfide) distances (2.519(4) and 2.565(4) Å) compare favorably with those observed (2.456(2)−2.531(1) Å, av 2.482 Å for 4 values)[46−48] in several distorted-octahedral Ni(II)−S(disulfide) complexes. The Ni−I (2.796(3) and 2.762(3) Å) and Ni−N(nitrile) (2.15(1) and 1.98(2) Å) distances may be similarly compared (Ni−I range, 2.720(1)−2.8381(19) Å;[49−53] Ni−N(nitrile) range, 2.032(18)[54]−2.193(7)[55] Å, av 2.086 Å for 42 values).

In viewing *meso*-**7**, *meso*-**8**, *meso*-**10**, and **17** as a group, we see that major structural differences lie in the M−S(disulfide) bond distances, reflecting the several coordination geometries, and in the C−S−S−C torsion angles (Table 2). The disulfide groups range from nonbonding in *meso*-**10** (one S atom) to weakly bonding in **17** to strongly bonding in *meso*-**7**, *meso*-**8**, and *meso*-**10** (the second S atom). Disulfide torsion angles range from 106.0(2) to 112.6(2)° for the free ligands *meso*-**9** and *rac*-**9** and for the relatively unconstrained disulfide groups in *meso*-

(42) Kwiatkowski, M.; Kwiatkowski, E.; Olechnowicz, A.; Bandoli, G.; Dolmella, A. *Inorg. Chim. Acta* **1992**, *201*, 177−84.
(43) Bhaduri, S.; Rugmini, V.; Sapre, N. Y.; Jones, P. G. *Acta Crystallogr.* **1996**, *C52*, 804−6.
(44) Nagle, P.; Hathaway, B. J. *Acta Crystallogr.* **1991**, *C47*, 1386−9.
(45) Basu, A.; Bhaduri, S.; Sapre, N. Y.; Jones, P. G. *J. Chem. Soc., Chem. Commun.* **1987**, 1724−5.
(46) Manzur, C.; Bustos, C.; Schrebler, R.; Carillo, D.; Knobler, C. B.; Gouzerh, P.; Jeannin, Y. *Polyhedron* **1989**, *8*, 2321−30.
(47) Warner, L. G.; Ottersen, T.; Seff, K. *Inorg. Chem.* **1974**, *13*, 2529−34.
(48) Warner, L. G.; Kadooka, M. M.; Seff, K. *Inorg. Chem.* **1975**, *14*, 1773−8.
(49) Endres, H. *Acta Crystallogr.* **1985**, *C41*, 1423−6.
(50) Sellmann, D.; Ruf, R.; Knoch, F.; Moll, M. *Z. Naturforsch.* **1995**, *50B*, 791−801.
(51) Bailey, N. A.; Fenton, D. E.; Kitchen, S. J.; Lilley, T. H.; Williams, M. G.; Tasker, P. A.; Leong, A. J.; Lindoy, L. F. *J. Chem. Soc., Dalton Trans.* **1991**, 627−37.
(52) Schrauzer, G. N.; Zhang, C.; Schlemper, E. O. *Inorg. Chem.* **1990**, *29*, 3371−6.
(53) Fitzpatrick, M. G.; Hanton, L. R. *Acta Crystallogr.* **1986**, *C42*, 1287−9.
(54) Søtofte, I.; Hazell, R. G.; Rasmussen, S. E. *Acta Crystallogr.* **1976**, *B32*, 1692−6.
(55) Zhong, Z. J.; Matsumoto, N.; Okawa, H.; Kida, S. *J. Chem. Soc., Dalton Trans.* **1989**, 2095−7.

10 and **17**. For *meso*-**7** and *meso*-**8**, they reduce to ca. 90.7(6)−94.6(2)°, presumably because of the relatively strong M−S(disulfide) bonds in these systems. The coordination geometries observed reflect both the flexibility of the macrocyclic ligands and the "plasticity" of the Cu(II) ion, where plasticity is taken to mean "the ability of the Cu(II) center to realize—with a given set of ligands—a variety of different coordination geometries with relatively small changes in thermodynamic stability."[56]

Syntheses

The tetradentate N_2S_2 ligand *rac*-**4** was prepared by reduction of the Schiff base precursor[19] *rac*-**3** using a synthetic route similar to that reported for related ligands.[18] Displacement of acetylacetone from $Ni(acac)_2$ using a slight excess of crude *rac*-**4** gave the NiN_2S_2 complex *rac*-**5** in good yield (Scheme 1).

Subsequent oxidation of *rac*-**5** with an equimolar quantity of I_2 afforded the novel binuclear Ni(II) complex **7**. Oxidative coupling of *rac*-**5** can yield *meso*-**7**, in which *meso*-**9** is the ligand, *rac*-**7**, in which *rac*-**9** is the ligand, or a mixture of both. The meso complex (see above) was isolated as green crystals whose structure revealed Ni(II) ions with a distorted-octahedral coordination geometry determined by equatorial N_2S_2 coordination from the macrocyclic ligand and axial coordination by acetonitrile and iodide. The reaction of a related sterically congested NiN_2S_2 complex with iodine gave a simple donor−acceptor $NiN_2S_2-I_2$ adduct (**23**) having an I−S contact of 2.601(4) Å.[57] A less sterically hindered NiN_2S_2 analogue reacted with I_2 to yield a trimetallic nickel complex (**24**) in which thiolate bridging involving two NiN_2S_2 units provided planar S_4 coordination for the third Ni(II) ion.[57] The N_2S_2 ligand displaced from the central Ni(II) was thought to be converted to a disulfide. The same trimetallic cation has been prepared with bromide counterions by the analogous oxidation with Br_2.[58] The green crystalline product from the reaction of *rac*-**5** with iodine was accompanied by small quantities of six-sided red plates, whose characterization revealed a second type of trimetallic nickel complex.[59]

The corresponding reaction of *rac*-**4** with $Cu(acac)_2$ gave the CuN_2S_2 complex *rac*-**6**,[20] another uncommon redox-stable bis(thiolato)Cu(II) complex.[60] Oxidation of *rac*-**6** with I_2 afforded *meso*-**8**, the isostructural Cu(II) analogue of the Ni(II) complex *meso*-**7**. Complex *meso*-**8** exhibits novel disulfide-bridged Cu(II) units and unusual redox-stable Cu(II)−iodide bonding. Because the expected disulfide → Cu(II) ligand-to-metal charge transfer (LMCT) absorptions of *meso*-**8** are difficult to identify in the presence of intense I → Cu(II) LMCT absorptions, we attempted to prepare Cu(II) complexes of **9** with additional coordination provided by ligands spectroscopically more innocent than iodide.

Facile demetalation of the binuclear Ni(II) complex *meso*-**7** was achieved by treatment of the complex with aqueous K_2CO_3. The free ligand was extracted into CH_2Cl_2. Slow evaporation of the dried CH_2Cl_2 solution yielded a mixture of square plates and clumps of prisms that were easily separated by hand in high total yield. Crystallographic studies revealed these phases to be the meso (*meso*-**9**) and rac (*rac*-**9**) isomers, respectively. These three isomers are expected from oxidative coupling of *rac*-**5**. Reaction of the free ligand *meso*-**9** with a solution containing Cu(II) and cyanate ions gave *meso*-**10** [Cu_2(*meso*-**9**)$(NCO)_4$], whose electronic spectrum is presented below (Figure 6).

Changing the macrocycle ring size may be expected to alter the coordination geometry of the binuclear metal ion units. A parallel synthetic route to a larger macrocycle (Scheme 2) was developed in which 2,2′-dimethyl-1,3-diaminopropane (**11**) was substituted for *trans*-*rac*-1,2-diaminocyclohexane. Here, complications arising from the presence of enantiomers were eliminated by the choice of a symmetrical diamine. Reduction of the Schiff base **12** gave the N_2S_2 ligand **13**. Displacement of acetylacetone from $Ni(acac)_2$ by using a slight excess of the reduction product **13** afforded the NiN_2S_2 complex **14**. Subsequent oxidation of **14** with an equimolar quantity of I_2 afforded the binuclear Ni(II) complex **15** of the potentially octadentate macrocyclic bis(disulfide)tetramine ligand **16**. Ligand **16** was obtained by stirring **15** with an acetonitrile/water mixture and was reacted with Cu(II) and cyanate, yielding complex **17**, [Cu_2(**16**)$(NCO)_4$·$2CH_3CN$].

Electronic Spectral Studies

Electronic spectra of ligands *meso*-**9** and *rac*-**9** are presented in Figure 4. Their lowest energy absorptions at ∼42 000 cm^{-1} are assigned to the first relatively weak Rydberg transition of the disulfide groups.[61] The second, more intense Rydberg transition arising from the disulfide groups contributes to the absorptions at ∼52 000 cm^{-1}. The first Rydberg transition of the secondary amine group has approximately $n_N \rightarrow$ 3s character[62,63] and is thought to account for the absorptions at ∼48 000 cm^{-1}. The second amine Rydberg transition has approximately $n_N \rightarrow$ 3p character and is thought to contribute to the highest energy absorptions at ∼52 000 cm^{-1}

As expected for a salt, *meso*-**7** has poor solubility in organic solvents (e.g., ∼0.7 mM at saturation in acetonitrile); consequently, solution studies of the relatively weak LF absorptions are not reported. However, deconvolution of the spectrum of *meso*-**7** dispersed in KBr (Supporting Information) reveals broad weak LF absorptions centered at approximately 10 600 and 17 600 cm^{-1}; the expected third LF absorption is masked by onset of the considerably more intense (∼100×) lowest energy LMCT absorption at ∼24 500 cm^{-1}. Despite the fairly low symmetry of this six-coordinate Ni(II) chromophore, apparent splittings[64] of the LF absorptions in the room-temperature mull spectrum were not observed. Deconvolution of the near-UV spectrum of the saturated acetonitrile solution (Figure 5) reveals overlapping LMCT absorptions at ∼25 500 (ϵ = ∼3000 *per Ni*(*II*)) and 28 100 cm^{-1} (ϵ = ∼3400 *per Ni*(*II*)) built on more intense absorptions at higher energies. Because of the probable

(56) Ammeter, J. H.; Bürgi, H. B.; Gamp, E.; Meyer-Sandrin, V.; Jensen, W. P. *Inorg. Chem*. **1979**, *18*, 733−50.
(57) Lyon, E. J.; Musie, G.; Reibenspies, J. H.; Darensbourg, M. Y. *Inorg. Chem*. **1998**, *37*, 6942−6.
(58) Farmer, P. J.; Solouki, T.; Mills, D. K.; Soma, T.; Russell, D. H.; Reibenspies, J. H.; Darensbourg, M. Y. *J. Am. Chem. Soc*. **1992**, *114*, 4601−5.
(59) A crystallographic study revealed this minor red phase to be a trimetallic Ni complex that differs from that described in refs 57 and 58. The central Ni species shows an unusual distorted NiS_2I_2 geometry. The presence of *three* iodine atoms (one lattice, one ligating iodide, and one apparently ligating iodonium that also bridges two thiolates) supports formulation of the central nickel as a Ni(I) species. Fox, S.; Stibrany, R. T.; Knapp, S.; Potenza, J. A.; Schugar, H. J. To be submitted for publication.
(60) Bharadwaj, P. K.; Potenza, J. A.; Schugar, H. J. *J. Am. Chem. Soc*. **1986**, *108*, 1351−2.
(61) Thompson, S. D.; Carroll, D. G.; Watson, F.; O'Donnell, M.; McGlynn, S. P. *J. Chem. Phys*. **1966**, *45*, 1367−79.
(62) Robin, M. B. *Higher Excited States of Polyatomic Molecules*; Academic Press: New York, 1974; Vol. 1, pp 208−19.
(63) Taylor, D. P.; Dion, C. F.; Bernstein, E. R. *J. Chem. Phys*. **1997**, *106*, 3512−8.
(64) Lever, A. B. P. *Inorganic Electronic Spectroscopy*, 2nd ed.; Elsevier: New York, 1984; pp 511−20.

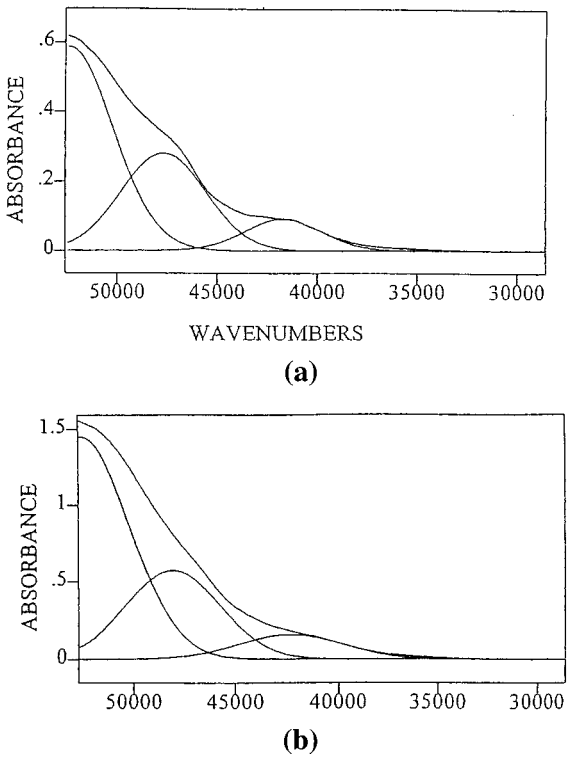

Figure 4. (a) Room-temperature spectrum of a 0.31 mM acetonitrile solution of *meso*-**9** (1.0 cm path length). Spectral deconvolution revealed absorptions at 41 700, 47 700, and 52 400 cm^{-1} having respective ϵ values of 300, 900, and 1900. (b) Spectrum of a 0.72 mM acetonitrile solution of *rac*-**9** (1.0 cm path length). Spectral deconvolution revealed absorptions at 42 900, 48 800, and 52 800 cm^{-1} having respective ϵ values of 220, 730, and 2000.

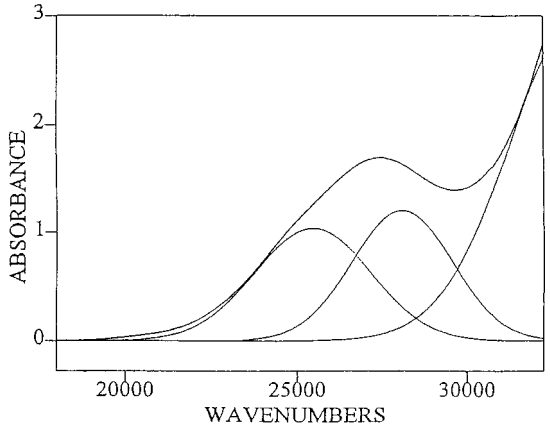

Figure 5. Room-temperature spectrum of a 0.70 mM acetonitrile solution of *meso*-**7** (1.0 cm path length). Spectral deconvolution revealed absorptions at 25 500, 30 700, and 28 100 cm^{-1} having respective ϵ values *calculated per Ni*(*II*) of 3000 and 3400.

overlap of the prominent $I^- \rightarrow$ Ni(II) LMCT absorptions with those originating from disulfide ligation, assignment of the UV spectrum was not pursued. Disulfide → Cu(II) LMCT absorptions of the isomorphous Cu(II) analogue *meso*-**8** are obscured for the same reason.

To circumvent the masking effect of iodide, *meso*-**10**, a second adduct of Cu(II) with *meso*-**9**, was prepared using cyanate for charge compensation. In *meso*-**10**, as noted above, the Cu(II) ions show approximately trigonal-bipyramidal N_4S coordination and the disulfide groups effectively have become nonbridging. The single Cu−S bond is equatorial, and the sulfur orbitals may be expected to enjoy only modest overlap with the (probable) d_{z^2} vacancy on Cu(II). Deconvolution of the

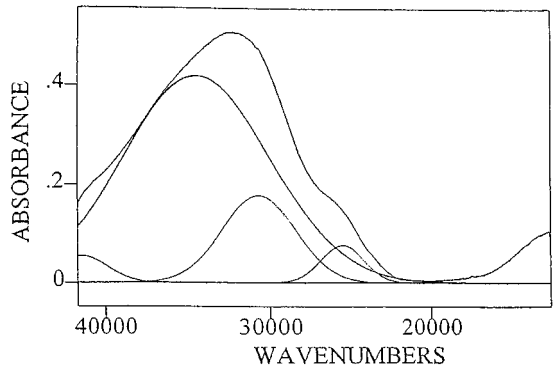

Figure 6. Room-temperature spectrum of a 0.754 mM dichloromethane solution (0.1 cm path length) of *meso*-**10**. Spectral deconvolution revealed absorptions at 11 800 (LF), 25 600, 30 700, 34 400, and 41 400 cm^{-1} having respective ϵ values *calculated per Cu*(*II*) of 700, 510, 1200, 2800, and 350.

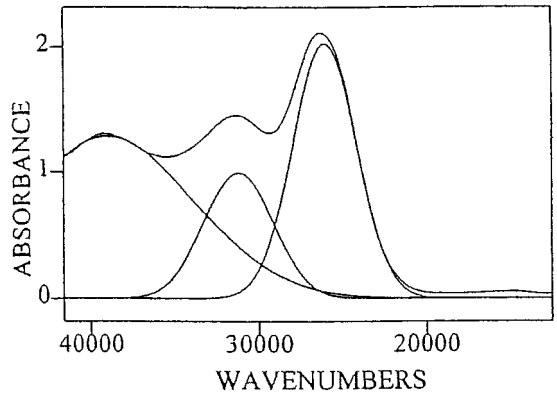

Figure 7. Room-temperature spectrum of a 0.447 mM dichloromethane solution (1.0 cm path length) of **17**. Spectral deconvolution revealed absorptions at 15 000 (LF), 26 100, 31 000, and 39 000 cm^{-1} having respective ϵ values *calculated per Cu*(*II*) of ∼20, 2300, 1100, and 1400.

solution electronic spectrum of *meso*-**10** (Figure 6) reveals ligand field absorption at 11 800 cm^{-1} along with four UV absorptions below the spectroscopic cutoff of methylene chloride. The mull spectrum of *meso*-**10** (Supporting Information) is similar to the solution spectrum, suggesting that the chromophore responsible for the latter spectrum is nearly the same as that in the solid state determined by X-ray crystallography. The UV spectrum of *meso*-**10** is similar in appearance to and red-shifted by ∼3000−4000 cm^{-1} from that of a reference CuN_5 chromophore[65] containing ligation supplied by the tetradentate N_4 ligand tris(2-aminoethyl)amine and a single apical cyanate. A portion of the red-shift in the LMCT spectrum of *meso*-**10** likely arises from stabilization of the resulting Cu(I) excited state by "soft" sulfur ligation. Compelling evidence for disulfide → Cu(II) LMCT absorptions in the spectrum of *meso*-**10** is absent, and the observed spectrum appears to be dominated by amine → Cu(II) and isocyanate → Cu(II) LMCT absorptions.

Finally, cyanate counterions also were used in the preparation of **17**, in which the Cu(II) ions show distorted N_4S_2 coordination with *both* Cu−S bonds being long and weak. Thus, any disulfide → Cu(II) LMCT absorptions are expected to be weak because of poor overlap of the sulfur orbitals with the Cu(II) d-vacancy. Ultraviolet absorptions (Figure 7) shown by **17** at 26 100, 31 000, and 39 000 cm^{-1}, having respective ϵ values *calculated per Cu*(*II*) of 2300, 1100, and 1400, appear to be dominated by amine → Cu(II) and isocyanate → Cu(II) LMCT, as with *meso*-**10**.

(65) Stibrany, R. T. Unpublished results.

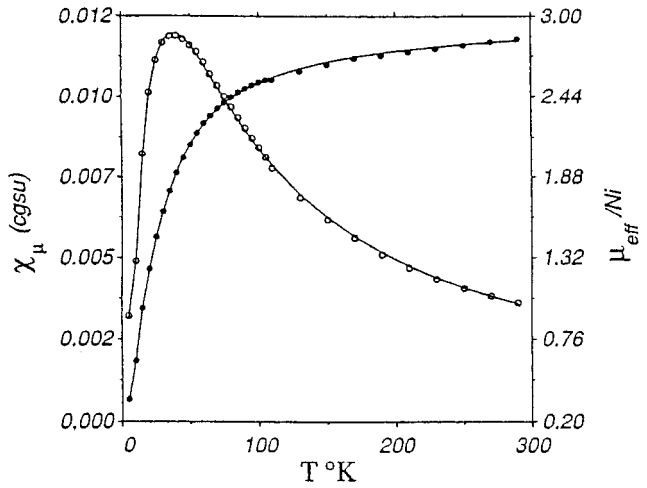

Figure 8. Temperature dependence of the measured magnetic susceptibility (χ, open circles) and magnetic moment (μ, solid circles) per mole of Ni(II) in *meso*-**7**. The curves were calculated by using the equation and parameters found in the text.

Magnetic Studies

The temperature-dependent magnetic susceptibility reported for a disulfide-bridged Ni(II) complex having additional bridging by two acetate groups (**25**) follows Curie−Weiss behavior [$\chi = C/(T - \theta)$] over the temperature range 100−300 K, with $\theta = -4$ K.[12] This result was interpreted as showing that magnetic interactions within this facially tris-bridged binuclear Ni(II) species are very weak.

In contrast, the dual disulfide-bridged Ni(II) unit in *meso*-**7** exhibits definitive antiferromagnetic behavior (Figure 8). The magnetic moment per Ni(II) decreases steadily from 2.86 μ_B at 290 K to 0.284 μ_B at 5 K, and the susceptibility passes through a maximum at about 40 K. The data were fit to a model based upon the usual $H = -2JS_1 \cdot S_2$ Hamiltonian including terms for interdimer interactions and zero field splitting.[66] Exploration of parameter space indicated that the best fit is obtained for $g = 2.06(2)$, $J = -13.0(2)$ cm^{-1}, and TIP = (130−300) × 10^{-6} cgs per Ni(II), while allowing for the presence of 0.6−1.1% monomeric Ni(II) impurity. Because of the strong correlation between the interdimer interaction (0.2 to −0.9 cm^{-1}) and zero field splitting (4.4−7.3 cm^{-1}), only the indicated ranges rather than absolute values can be determined using this approach.[67]

Depending upon the orbital pathways, ligand-bridged binuclear Ni(II) complexes can show either antiferromagnetic or ferromagnetic coupling.[68] The extent of antiferromagnetic coupling exhibited by *meso*-**7** is considerable and exceeds that typically reported for Ni(II) ions doubly bridged by ligands such as Cl^-, Br^-, NCS^-, NCO^-, and NO_2^-,[68] demonstrating that bridging disulfide groups can provide substantial superexchange pathways. In *meso*-**10**, the disulfide groups do not effectively bridge the binuclear Cu(II) unit (see above); consequently, *meso*-**10** shows a magnetic moment per Cu(II) that decreases slowly from 1.67 μ_B at 290 K to 1.60 μ_B at 5 K. The data can be fit to the usual dimer model with $g = 1.91$, $J = 0.52$ cm^{-1}, and TIP = 44 × 10^{-6} cgsu, with 0.3 wt % of paramagnetic Cu(II) impurity.

Conclusions

Ni(II) and Cu(II) complexes of linear tetradentate N_2S_2 diaminodithiolate ligands are oxidatively coupled with I_2 in an efficient manner to yield binuclear complexes of novel macrocyclic bis(disulfide)tetramines. Facile demetalation of the Ni(II) oxidation products affords the free macrocyclic ligands. Crystallographic studies reveal that, depending upon the size of the macrocyclic ligand and the nature of the additional ligands (I^-, NCO^-, and CH_3CN), the Cu(II) coordination geometry shows considerable plasticity with concomitant changes in the details of Cu(II)−disulfide bonding. Thus, a diiodide salt contains six-coordinate Cu(II) in which all four bridging disulfide sulfur atoms are equatorially bound. In contrast, the isocyanato salts of the 16- and 18-membered macrocycles exhibit trigonal-bipyramidal Cu(II) and distorted cis-octahedral Cu(II) geometries, respectively, having only one and no short equatorially bound sulfurs. Disulfide → Cu(II) LMCT absorptions of these isocyanato-containing Cu(II) species appear to be too weak to observe, probably because of poor overlap of the sulfur orbitals with the Cu(II) d-vacancy. The dual disulfide-bridged Ni(II) units of the crystallographically characterized Ni(II) complex *meso*-**7** promote substantial antiferromagnetic coupling.

Supporting Information Available: Spectrum of *meso*-**7** dispersed in KBr; mull spectrum of *meso*-**10**; tables of crystal structure and refinement details, atomic coordinates, anisotropic thermal parameters, and bond lengths and angles for the several structures. This material is available free of charge via the Internet at http://pubs.acs.org.

IC000380P

(66) Ginsberg, A. P.; Martin, R. L.; Brookes, R. W.; Sherwood, R. C. *Inorg. Chem.* **1972**, *11*, 2884−9.

(67) The least-squares fitting program was obtained from Professor C. J. O'Connor, Department of Chemistry, University of New Orleans.

(68) Sacconi, L.; Mani, F.; Bencini, A. In *Comprehensive Coordination Chemistry*; Wilkinson, G., Ed.; Pergamon: New York, 1987; Vol. 5, pp 277−83.